



## Link between volume, thermal expansion, and bulk metallic glass formability

A. K. Gangopadhyay ,\* C. E. Pueblo, and K. F. Kelton 

*Department of Physics, Washington University in St. Louis, St. Louis, Missouri 63130, USA*



(Received 20 May 2020; revised 14 August 2020; accepted 31 August 2020; published 16 September 2020)

The specific volumes and thermal expansion coefficients of 41 transition-metal based alloy liquids, which include both bulk and marginal glass-formers, are presented. Those parameters are compared with their values either in the corresponding crystal phases or in their constituent elemental liquids. The volume differences in both cases at the liquidus temperature,  $T_l$ , correlate well with the critical thicknesses,  $d_{\text{crit}}$  of the corresponding glass, taken either from literature or from estimates. The estimates are based on a recent study [Dai *et al.*, *J. Non-Cryst. Solids* **525**, 119673 (2019)], which requires knowledge of the liquid expansion coefficient and viscosity. The volume differences between the better glass-forming liquids and the crystal phases are smaller; they are larger when compared with the elemental liquids. The thermal expansion coefficients of the liquids correlate well with the cohesive energies and fragilities. Their differences with the crystal phases and estimates from elemental liquids correlate well with  $d_{\text{crit}}$ . The differences are *smaller* for the former and *larger* for the latter for alloy liquids having larger values of  $d_{\text{crit}}$ . This parameter then appears to be a prime indicator of glass formability. The results are explained in terms of changes in the anharmonicity and structural contributions to the expansion coefficients on alloying.

DOI: [10.1103/PhysRevMaterials.4.095602](https://doi.org/10.1103/PhysRevMaterials.4.095602)

### I. INTRODUCTION

Since the first discovery of a metallic glass (MG) [1], the dense random-packing (DRP) model [2] has been one of the most used structural models. It has found support in more recent studies on the bulk metallic glasses (BMG, with critical thickness more than 1 mm) from computer simulations [3,4] and phenomenological models [5]. According to these studies, the basic structural motifs of solute-centered clusters pack efficiently to form the BMGs. It is then expected that the packing densities of the better glass-forming liquids and glasses should be higher compared to those for the poorer glass formers. The glass-formability parameter, GFA, is usually measured in terms of the critical casting thickness,  $d_{\text{crit}}$ , or the critical cooling rate that is necessary to form a glass from the corresponding liquid. Larger densities for the better glass formers were reported in a series of Cu-Zr glasses [6]. However, when such measurements were extended to the liquids of the same alloys, no such correlation was observed [7]. Similar conflicting results emerged when the densities/volumes of the liquids/glasses were compared with the values in the corresponding crystal phases. The density difference between the crystal and glass near the crystallization temperature,  $T_x$ , was found to be larger in Cu-Zr glasses with a larger  $d_{\text{crit}}$  (better GFA) [6]. In contrast, near the melting temperature,  $T_l$ , the difference was smaller for larger  $d_{\text{crit}}$  in other BMGs [8]. This naturally raises a question of why the two results are opposite to each other at two different characteristic temperatures. After all, the glass is also a liquid, although a metastable and frozen one.

Another important unexplained issue is the correlation between the liquid thermal expansion coefficient,  $\alpha_{\text{liq}}$ , and GFA. A larger  $\alpha_{\text{liq}}$  was observed for the better glass formers in the Cu-Zr glasses [7], whereas an opposite correlation became apparent when many different types of metallic liquids were considered [9]. This is a motivation to undertake a more comprehensive analysis of the densities/volumes and thermal expansion coefficients of the liquids and their corresponding crystals. Since the differences in those properties are usually small, measurements by the same group of investigators using the same experimental technique is desirable, so that the systematic errors in the measurements remain similar for all alloys.

This study is focused on testing some of the expectations from the DRP model and resolving the discrepancies in the published results. The thermodynamic properties under consideration, the volumes and thermal expansion coefficients of 41 alloy liquids measured over several years by our group, are presented and analyzed. The liquids include good, marginal, and poor glass formers. The absolute values of the thermodynamic properties are unimportant when comparing alloys containing different elements. Instead, a meaningful comparison of the difference with some baseline is required. The liquid properties may be compared with those of the corresponding glass or crystal phase. They may also be compared with the estimated values from the properties of the elemental liquids that constitute the alloy. The differences from the baseline values may then be correlated with  $d_{\text{crit}}$ . The differences in both the volume and thermal expansion coefficients with those baselines have been found to correlate well with the GFA and the trend is reflected more prominently in the thermal expansion coefficient than in the specific volume/density.

\*anup@wuphys.wustl.edu

## II. EXPERIMENTAL PROCEDURES

A noncontact electrostatic levitation technique was used to levitate, melt, and crystallize small spherical ( $\sim 2.5$ -mm diameter) samples under high vacuum ( $\sim 10^{-7}$  Torr), as described elsewhere [10,11]. Briefly, such samples were made from a master ingot ( $\sim 1$  g) by arc melting high-purity (greater than 3 N) elements in a high-purity (5 N)  $\text{Ti}_{50}\text{Zr}_{50}$ -gettered argon atmosphere. The density/specific volumes of the levitated samples were obtained from the analysis of two-dimensional video images [12,13]. The levitated liquid samples were approximately spherical due to surface tension, with very little distortion because of their small masses; some shape distortion occurred, however, after crystallization. Data from many cooling cycles were averaged to improve the statistics. The precision in the absolute value of density/volume is estimated to be about 1%, which is determined by the Tungsten Carbide (WC) standard used for calibration. The precision in the thermal expansion coefficient is about 3%. However, the relative changes can be measured with a much better precision by data averaging, better than 0.05% for the liquids and about 0.3% for the solids. The shear viscosity, which is necessary to estimate the critical thickness [14] and fragility [15], was obtained from the decay times of free oscillations induced in the droplets [16]. The  $T_g$ s of the glasses were measured by the differential calorimetry technique during heating at 20 °C/min.

## III. RESULTS

### A. Specific volumes

Tables I and II summarize all experimentally measured and estimated parameters used in the analyses. This includes measured specific volumes and thermal expansion coefficients of the liquids and corresponding crystal phases at  $T_l$  and the corresponding estimated values. Table II provides the experimental and estimated  $T_g$ s, along with the literature data and estimated values for  $d_{\text{crit}}$ . For a broader comparison, many marginal glass formers are included. However, since many of them do not show a clear signature for  $T_g$ , it was necessary to use estimated values. It has been recently shown that the  $T_g$  for the transition-metal based glasses [17] and some of the elemental liquids [18], may be estimated from the high-temperature thermodynamic and dynamic properties of the equilibrium liquids above or near  $T_l$ . The necessary parameters are the thermal expansion coefficient of the liquid,  $\alpha_{\text{liq}}$ , the dynamic crossover temperature,  $T_A$ , and another temperature,  $T^*$ , at which the viscosities of all liquids are the same. Accordingly, the  $T_g$  of the transition-metal based glasses are given by the empirical relation [17]

$$T_g = \frac{1920\alpha_{\text{liq}} + 0.297}{\frac{1}{T^*} - \frac{0.307}{T_A}}. \quad (1)$$

Here,  $T^*$  represents the temperature at which the viscosity for all the liquids is 60 mPa s. This choice has no physical significance but is a matter of convenience since experimental data for all the liquids studied are available at this particular value. If a different value of the viscosity were chosen, the numerical parameters in Eq. (1) will change accordingly. As shown in Table II, the estimated values of  $T_g$  obtained from the

liquids using Eq. (1) agree with the measured  $T_g$  in the glass to within 1–3%.

The  $T_A$  has been recently recognized as an important temperature for glass formation [19–23]. Although it is well known that the viscosity changes from a high-temperature Arrhenius form [ $\eta = \eta_0 \exp(E/k_B T)$ , where  $k_B$  is the Boltzmann constant and  $E$  a characteristic activation energy for flow], to a non-Arrhenius form (where  $E$  becomes temperature dependent), the physical significance of this crossover temperature has been understood only recently. Both from measurements and molecular-dynamic simulations, it is identified as the temperature below which local structural rearrangements become cooperative. It has another practical importance, however. Experimentally, the fragility is usually determined from viscosity measurements made near  $T_g$  [ $m = d \log \eta / d(T_g/T)$  at  $T_g$ ] [15]. However, for the marginal glass formers rapid crystallization upon approaching  $T_g$  makes such measurements extremely difficult. Alternatively, fragility can be determined from the ratio  $T_A/T_g$  [22] and  $T^*/T_g$  [9,23], which are much more convenient to measure for the marginal glasses. Stronger liquids show larger values of  $T_A/T_g$  [22] and  $T^*/T_g$  [9,23].

The critical casting thickness,  $d_{\text{crit}}$ , for the glasses can be often improved by using special processing techniques, such as fluxing [24]. However, since very few BMGs have been produced by this method, to make the comparisons meaningful, data obtained only from normal processing methods, such as casting in silica tubes or Cu molds, are included for the analysis. For many alloys in the present study, no experimental data exist for  $d_{\text{crit}}$ . Johnson *et al.* [25] established an empirical relationship between  $d_{\text{crit}}$ , the reduced glass transition temperature,  $T_{rg} = T_g/T_l$ , and fragility. However, to estimate  $d_{\text{crit}}$  by this method, the fragility must be measured, which is a very difficult proposition for the marginal and poor glass formers, as discussed earlier. Recently, our group modified Johnson's method to use parameters obtained from the high-temperature liquid [14]. The empirical relationship used to determine  $d_{\text{crit}}$  is

$$\log[d_{\text{crit}}^2(\text{mm})] = 7.232 + \frac{26168\alpha_{\text{liq}} + 4.048}{T_l/T^* - 0.307T_l/T_A} - \frac{43960\alpha_{\text{liq}} + 6.8}{1 - 0.307T^*/T_A}. \quad (2)$$

According to Eq. (2), it is not necessary to first make the glass and then measure its value of  $T_g$  to make this estimate. Table II includes the viscosity parameters and estimated values of  $d_{\text{crit}}$ , along with the literature data when available.

Figure 1 shows the changes in volume for 15 alloys upon melting (differences between the specific volumes of the liquid and crystal at  $T_l$ ) as a function of  $d_{\text{crit}}$  values from the literature. The corresponding measured data are listed in Table I. Significant scatter in the data is visible, mostly because of imprecise measurements of the crystal volumes due to distortions of the levitated liquid drops on crystallization. Since the typical changes in volume on melting are small, high-precision data are required. In spite of the scatter, Fig. 1 shows that the volume changes are smaller for the better glass formers (larger  $d_{\text{crit}}$ ). The two outliers are alloy numbers 37 (Vit106) and 38 (Vit106a). It is possible that because these are multicomponent alloys (five elements), the correlation

TABLE I. The liquidus temperature  $T_l$ , the corresponding experimentally measured and estimated specific volumes of the liquids,  $V_{liq}$ , and measured crystal volumes,  $V_{cryst}$  are shown below. The measured liquid and crystal expansion coefficients,  $\alpha_{liq}$  and  $\alpha_{cryst}$ , as well as the estimated values of  $\alpha_{liq}$  using the mixing rule for the elemental liquids are also included. The data for the elemental liquids are taken from the literature.

Alloy number	Composition	$T_l$ (K)	Measured $V_{liq}$ ( $\text{cm}^3/\text{g}$ ) at alloy $T_l$	Measured $V_{cryst}$ ( $\text{cm}^3/\text{g}$ ) at alloy $T_l$	Estimated $V_{liq}$ ( $\text{cm}^3/\text{g}$ ) at alloy $T_l$	Estimated $V_{liq}$ ( $\text{cm}^3/\text{g}$ ) at elemental $T_l$	Measured $\alpha_{liq}$ ( $10^{-5}$ )	Measured $\alpha_{cryst}$ ( $10^{-5}$ )	Estimated $\alpha_{liq}$ ( $10^{-5}$ )
1	Co <sub>50</sub> Pd <sub>50</sub>	1492	0.11006		0.10615	0.10934	8.40(0.15)		9.58
2	Co <sub>70</sub> Pd <sub>30</sub>	1513	0.10948		0.11225	0.11556	8.45(0.37)		10.53
3	Co <sub>80</sub> Pd <sub>20</sub>	1544	0.11489		0.11561	0.11866	9.71(0.16)		11.01
4	Cu <sub>28</sub> Zr <sub>72</sub>	1267	0.14793		0.14667	0.15142	5.72(0.08)		5.99
5	Cu <sub>46</sub> Zr <sub>54</sub>	1198	0.14347	0.1407	0.14032	0.14482	6.26(0.1)	3.33(0.1)	6.98
6	Cu <sub>50</sub> Zr <sub>50</sub>	1222	0.14051		0.13927	0.14335	6.7(0.1)		7.2
7	Cu <sub>56</sub> Zr <sub>44</sub>	1200	0.13895		0.13713	0.14115	7.43(0.1)		7.53
8	Cu <sub>64</sub> Zr <sub>36</sub>	1200	0.13348		0.13457	0.13821	7.82(0.1)		7.97
9	Cu <sub>50</sub> Zr <sub>42.5</sub> Ti <sub>7.5</sub>	1152	0.14466	0.14223	0.14368	0.14913	7.30(0.1)	3.64(0.07)	7.50
10	Cu <sub>60</sub> Zr <sub>30</sub> Ti <sub>10</sub>	1235	0.1418		0.14316	0.14738	8.05		8.16
11	Cu <sub>60</sub> Zr <sub>20</sub> Ti <sub>20</sub>	1127	0.1440	0.14127	0.14863	0.15508	8.26(0.2)	4.48(0.1)	8.56
12	Cu <sub>50</sub> Zr <sub>45</sub> Al <sub>5</sub>	1173	0.14485	0.14256	0.15261	0.1562	7.18(0.12)	3.70(0.1)	7.61
13	Cu <sub>47</sub> Zr <sub>47</sub> Al <sub>6</sub>	1180	0.14633	0.14374	0.15637	0.15987	6.91(0.17)	3.45(0.09)	7.52
14	Cu <sub>47</sub> Zr <sub>45</sub> Al <sub>8</sub>	1163	0.14746	0.14469	0.16171	0.16501	6.80(0.1)	3.56(0.1)	7.69
15	Cu <sub>46</sub> Zr <sub>42</sub> Y <sub>7</sub> Al <sub>5</sub>	1113	0.15078		0.16257	0.16677	7.43(0.19)		7.58
16	Pd <sub>82</sub> Si <sub>18</sub>	1081	0.1004		0.13885	0.14735	6.67(0.15)		7.76
17	Ti <sub>50</sub> Zr <sub>50</sub>	1823	0.18857		0.19789	0.2002	5.26(0.06)		6.48
18	Ti <sub>39.5</sub> Zr <sub>39.5</sub> Ni <sub>21</sub>	1093	0.16892		0.17389	0.18512	5.05(0.06)		6.94
19	Ti <sub>34</sub> Zr <sub>11</sub> Cu <sub>47</sub> Ni <sub>8</sub> (Vit101)	1164	0.15083		0.16021	0.16797	7.76		8.75
20	Ti <sub>45</sub> Zr <sub>45</sub> Ni <sub>10</sub>	1543	0.17606		0.18728	0.19303	4.82		6.70
21	Ti <sub>40</sub> Zr <sub>10</sub> Cu <sub>36</sub> Pd <sub>14</sub>	1185	0.14946	0.14693	0.16157	0.16978	7.27(0.14)	3.94(0.19)	8.44
22	Ti <sub>40</sub> Zr <sub>10</sub> Cu <sub>30</sub> Pd <sub>20</sub>	1189	0.14601		0.15964	0.16791	7.51(0.11)		8.27
23	Y <sub>68.9</sub> Co <sub>31.1</sub>	988	0.15213		0.19440	0.20486	6.08		7.23
24	Zr <sub>57</sub> Ni <sub>43</sub>	1433	0.14428		0.14313	0.14738	5.22		6.28
25	Zr <sub>64</sub> Ni <sub>36</sub>	1283	0.14584		0.14405	0.14971	4.61(0.05)		5.98
26	Zr <sub>76</sub> Ni <sub>24</sub>	1233	0.14884		0.1475	0.15371	4.62(0.14)		5.47
27	Zr <sub>56</sub> Co <sub>28</sub> Al <sub>16</sub>	1241	0.15918		0.18934	0.19251	5.31		7.86
28	Zr <sub>60</sub> Ni <sub>25</sub> Al <sub>15</sub>	1248	0.16031	0.15909	0.18431	0.19193	4.87(0.11)	2.94(0.03)	6.74
29	Zr <sub>64</sub> Ni <sub>25</sub> Al <sub>11</sub>	1212	0.15735	0.15483	0.17438	0.18165	5.1(0.19)	3.17(0.15)	6.41
30	Zr <sub>70</sub> Pd <sub>30</sub>	1350	0.13345		0.13646	0.14133	4.65		5.28

TABLE I. (Continued.)

Alloy number	Composition	$T_l$ (K)	Measured $V_{liq}$ ( $\text{cm}^3/\text{g}$ ) at alloy $T_l$	Measured $V_{crist}$ ( $\text{cm}^3/\text{g}$ ) at alloy $T_l$	Estimated $V_{liq}$ ( $\text{cm}^3/\text{g}$ ) at alloy $T_l$	Estimated $V_{liq}$ ( $\text{cm}^3/\text{g}$ ) at elemental $T_l$	Measured $\alpha_{liq}$ ( $10^{-5}$ )	Measured $\alpha_{crist}$ ( $10^{-5}$ )	Estimated $\alpha_{liq}$ ( $10^{-5}$ )
31	Zr <sub>75.5</sub> Pd <sub>24.5</sub>	1303	0.138 16		0.140 07	0.145 06	4.73		5.12
32	Zr <sub>74</sub> Rh <sub>26</sub>	1415	0.135 67		0.138 52	0.143 69	4.38		5.11
33	Zr <sub>80</sub> Pt <sub>20</sub>	1449	0.119 73		0.135 58	0.139 78	4.36		4.56
34	Zr <sub>82</sub> Ir <sub>18</sub>	1513	0.122 97		0.137 59	0.141 65	4.29		4.41
35	Zr <sub>51</sub> Cu <sub>36</sub> Al <sub>9</sub> Ni <sub>4</sub> (LM601)	1157	0.150 45		0.164 53	0.170 29	6.33		7.33
36	Zr <sub>52.5</sub> Cu <sub>17.9</sub> Ni <sub>14.6</sub> Al <sub>10</sub> Ti <sub>5</sub> (Vit105)	1093	0.155 27	0.154 13	0.172 59	0.179 82	5.65(0.05)	3.55(0.22)	7.07
37	Zr <sub>57</sub> Cu <sub>15.4</sub> Ni <sub>12.6</sub> Al <sub>10</sub> Nb <sub>5</sub> (Vit106)	1123	0.152 80	0.150 34	0.171 04	0.175 98	5.20(0.07)	3.28(0.12)	6.69
38	Zr <sub>58.5</sub> Cu <sub>15.6</sub> Ni <sub>12.8</sub> Al <sub>10.3</sub> Nb <sub>2.8</sub> (Vit106a)	1125	0.153 84	0.152 17	0.172 54	0.177 3	5.17(0.10)	3.11(0.06)	6.71
39	Zr <sub>59</sub> Cu <sub>20</sub> Al <sub>10</sub> Ni <sub>8</sub> Ti <sub>3</sub>	1170	0.156 2	0.154 42	0.175 14	0.179 71	4.98(0.10)	2.96(0.03)	6.83
40	Zr <sub>62</sub> Cu <sub>20</sub> Al <sub>10</sub> Ni <sub>8</sub>	1241	0.155 58	0.153 88	0.173 10	0.177 4	5.33(0.05)	3.13(0.06)	6.71
41	Zr <sub>65</sub> Cu <sub>17.5</sub> Al <sub>7.5</sub> Ni <sub>10</sub>	1350	0.153 78	0.152 02	0.166 67	0.171 22	4.97(0.06)	2.99(0.05)	6.45
42	Al	933	0.418 7				12.6 [44,45]		
43	Co	1768	0.124 88				11.96 [46]		
44	Cu	1356	0.125 0				9.95 [47,48]		
45	Ir	2683	0.050 33				4.2 [49]		
46	Nb	2741	0.130 2				5.0 [50]		
47	Ni	1726	0.128 4				8.7 [50]		
48	Pd	1827	0.093 8				7.2 [51]		
49	Pt	2045	0.052 08				5.0 [49]		
50	Rh	2238	0.092 42				7.0 [51]		
51	Si	1683	0.391 32				10.3 [46,52]		
52	Ti	1943	0.238 7				8.5 [53,54]		
53	Zr	2125	0.161 7				4.45 [50,54]		
54	Y	1795	0.240 96				5.10 [55]		

TABLE II. Dynamical properties of the liquids used in the analysis are listed below. They include the temperature,  $T^*$  at which the viscosity is 0.06 Pa s, the crossover temperature,  $T_A$ , measured and estimated glass transition temperature,  $T_g$ , literature data, and estimated critical thickness,  $d_{\text{crit}}$ .

Alloy number	Composition	$T^*$ (K) $\eta = 6 \text{ mPa s}$	$T_A$ (K)	Measured $T_g$ (K)	Estimated $T_g$ (K)	$d_{\text{crit}}$ (mm) Literature	$d_{\text{crit}}$ (mm) Estimated
1	Co <sub>50</sub> Pd <sub>50</sub>						
2	Co <sub>70</sub> Pd <sub>30</sub>						
3	Co <sub>80</sub> Pd <sub>20</sub>						
4	Cu <sub>28</sub> Zr <sub>72</sub>						
5	Cu <sub>46</sub> Zr <sub>54</sub>	1080	1128	646	638	2 [56]	3
6	Cu <sub>50</sub> Zr <sub>50</sub>	1109	1196	677	660	2 [57]	3
7	Cu <sub>56</sub> Zr <sub>44</sub>	1115	1118	701	707	1 [6]	2.4
8	Cu <sub>64</sub> Zr <sub>36</sub>	1126	1249	739	699	2 [58,59]	3
9	Cu <sub>50</sub> Zr <sub>42.5</sub> Ti <sub>7.5</sub>	1067	1181	669	645	5 [60]	3.2
10	Cu <sub>60</sub> Zr <sub>30</sub> Ti <sub>10</sub>			700 [64]		4 [61]	
11	Cu <sub>60</sub> Zr <sub>20</sub> Ti <sub>20</sub>	1099	1219	679	692	4 [61]	3.9
12	Cu <sub>50</sub> Zr <sub>45</sub> Al <sub>5</sub>	1128	1241	695	680	3 [62]	4
13	Cu <sub>47</sub> Zr <sub>47</sub> Al <sub>6</sub>	1143	1222	695	689	6 [63]	4.7
14	Cu <sub>47</sub> Zr <sub>45</sub> Al <sub>8</sub>	1170	1335	677	684		9
15	Cu <sub>46</sub> Zr <sub>42</sub> Y <sub>7</sub> Al <sub>5</sub>			670 [67]		10 [64]	
16	Pd <sub>82</sub> Si <sub>18</sub>	1042	1287	634	589	3 [65]	7
17	Ti <sub>50</sub> Zr <sub>50</sub>						
18	Ti <sub>39.5</sub> Zr <sub>39.5</sub> Ni <sub>21</sub>						
19	Ti <sub>34</sub> Zr <sub>11</sub> Cu <sub>47</sub> Ni <sub>8</sub> (Vit101)	1111	1190	675	695	4 [66]	3.5
20	Ti <sub>45</sub> Zr <sub>45</sub> Ni <sub>10</sub>						
21	Ti <sub>40</sub> Zr <sub>10</sub> Cu <sub>36</sub> Pd <sub>14</sub>	1085	1239	642	648	6 [67]	3.2
22	Ti <sub>40</sub> Zr <sub>10</sub> Cu <sub>30</sub> Pd <sub>20</sub>	1119	1235	670	684	3 [67]	3.5
23	Y <sub>68.9</sub> Co <sub>31.1</sub>	1007			560		
24	Zr <sub>57</sub> Ni <sub>43</sub>	1200	1361		654		3.1
25	Zr <sub>64</sub> Ni <sub>36</sub>	1150	1265		623		5.8
26	Zr <sub>76</sub> Ni <sub>24</sub>	1085	1170		585		4.7
27	Zr <sub>56</sub> Co <sub>28</sub> Al <sub>16</sub>	1315	1402	738	737	18 [68]	17.7
28	Zr <sub>60</sub> Ni <sub>25</sub> Al <sub>15</sub>	1250	1355	688	681	15 [69]	12.5
29	Zr <sub>64</sub> Ni <sub>25</sub> Al <sub>11</sub>	1223	1290	669	681	12 [69]	11.7
30	Zr <sub>70</sub> Pd <sub>30</sub>	1195	1285		646		4.9
31	Zr <sub>75.5</sub> Pd <sub>24.5</sub>	1175	1260		641		5.4
32	Zr <sub>74</sub> Rh <sub>26</sub>	1264	1345		677		5.6
33	Zr <sub>80</sub> Pt <sub>20</sub>	1418	1660		732		14
34	Zr <sub>82</sub> Ir <sub>18</sub>	1337	1610		682		7.1
35	Zr <sub>51</sub> Cu <sub>36</sub> Al <sub>9</sub> Ni <sub>4</sub> (LM601)	1168	1320	694	671		9.8
36	Zr <sub>52.5</sub> Cu <sub>17.9</sub> Ni <sub>14.6</sub> Al <sub>10</sub> Ti <sub>5</sub> (Vit105)	1199	1305	672	677	18 [25]	23.5
37	Zr <sub>57</sub> Cu <sub>15.4</sub> Ni <sub>12.6</sub> Al <sub>10</sub> Nb <sub>5</sub> (Vit106)	1220	1349	671	670	20 [25]	25
38	Zr <sub>58.5</sub> Cu <sub>15.6</sub> Ni <sub>12.8</sub> Al <sub>10.3</sub> Nb <sub>2.8</sub> (Vit106a)	1195	1310	668	658	32 [25]	20
39	Zr <sub>59</sub> Cu <sub>20</sub> Al <sub>10</sub> Ni <sub>8</sub> Ti <sub>3</sub>	1162	1282	653	632	13 [70]	14
40	Zr <sub>62</sub> Cu <sub>20</sub> Al <sub>10</sub> Ni <sub>8</sub>	1180	1314	655	651	14 [70]	15
41	Zr <sub>65</sub> Cu <sub>17.5</sub> Al <sub>7.5</sub> Ni <sub>10</sub>	1169	1230	635	648	16 [71]	11

fails when several crystal phases form. Strictly speaking, the correlation should hold when the crystal and glass have the same chemical composition (polymorphic transformation). A straight-line fit without those two data are shown in Fig. 1 with an  $R^2 = 0.76$ . The correlation with  $d_{\text{crit}}$  for the 15 BMGs is in agreement with the earlier report on four BMGs [8] and meets the expectation from the DRP model. Because of the better packing of atoms in the better glass formers, their volumes are closer to those of the corresponding crystals. However, they contradict the findings reported in Ref. [6], where the volume changes during crystallization were found to be larger for the better glass formers. This point could not be clarified since the volume changes during glass crystallization are smaller

(typically, less than 1%), than the precision of the present measurements.

To gain additional insight from the volumetric data, the specific volume of the liquids at  $T_l$ , estimated from a simple rule of mixing of the elemental liquids, was chosen as another baseline. Accordingly, the expected specific volume is  $\sum_i c_i v_i$ , where  $c_i$  and  $v_i$  are the molar concentrations and the specific volumes of the  $i$ th elemental liquid, respectively. They were estimated from the literature data for the elemental liquids, as listed in Table I. Because of the large differences in  $T_l$  between the alloys and their constituent elements, it is proper that they should be estimated at the alloy  $T_l$ . However, for completeness, estimates at both alloy and elemental  $T_l$  are

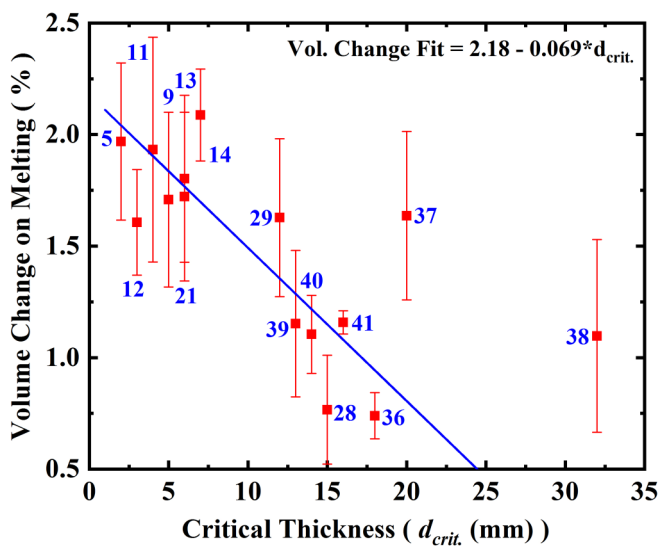


FIG. 1. The volume changes on melting of the crystals of some BMGs are compared with the literature values for critical thickness ( $d_{crit}$ ). The alloy numbers are the same as in Tables I and II. A linear fit excluding the alloy numbers 36 and 37 are also shown.

included in Table I. To include as many data points as possible, the differences between the measured and estimated specific volumes were then compared with the estimated values for  $d_{crit}$  from Eq. (2) for those alloys for which the viscosity was measured and reliable  $T^*$  and  $T_A$  parameters could be determined from the experimental data. The alloy numbers 1–4, 10, 15–18, 20, and 23 are excluded for those reasons.

The estimated values for  $d_{crit}$  are provided in Table II, which agree with the literature data within 10–20% in most cases; some larger disagreements are also observed. For example, the binary Zr-Ni (24,25), Zr-Pd (30,31), Zr-Rh (32), and Zr-Pt (33), Zr-Ir (34) alloys are marginal glass formers, which can be produced only in thin ribbon forms by rapidly quenching the liquids. In contrast our empirical expression identifies them as BMGs. One possible explanation is that the thermodynamic data for the liquids/glasses are not sufficient to predict  $d_{crit}$  for these alloys, as discussed in Ref. [14]. It was pointed out that missing information on the liquid and crystal structures may be needed. It was suggested a while ago [26] that when the local structures of the liquid and underlying crystal phase are similar, structural order in the liquid may act as a template that expedites nucleation. More recent data support this view [14]. It is not clear, however, how such structural information could be included to make a better model for the prediction of  $d_{crit}$ .

Figure 2 shows the differences between the measured and estimated volumes from the elemental liquids at the alloy  $T_l$  as a function of estimated critical thicknesses. The differences are negative (smaller alloy volumes) for most of the alloys; they become larger with increasing critical thicknesses. Following Inoue’s suggestion [27], many of the BMGs were discovered in alloys with large negative heats of mixing (attractive chemical interactions) [28]. Therefore, the experimental specific volumes are expected to be smaller than the estimates from the rule of mixing for the glass-forming liquids, as observed. A polynomial fit to the data is given by the

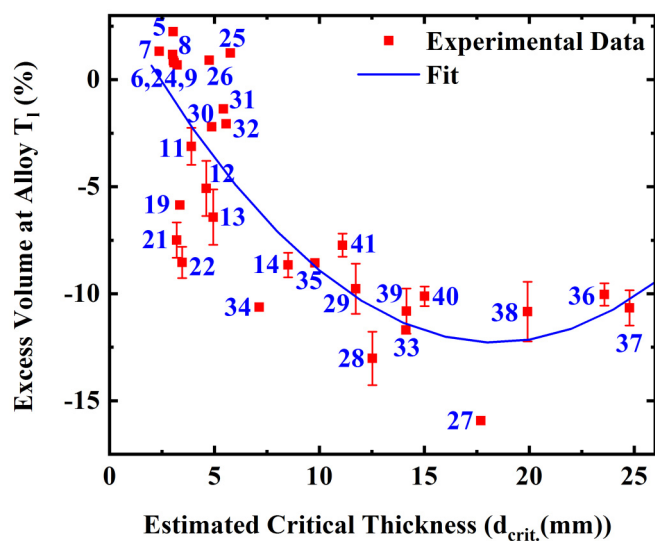


FIG. 2. The measured volume of the liquid at  $T_l$  in excess of the estimated volume from the elemental liquids at the  $T_l$  of the alloys. The alloy numbers are the same as listed in Tables I and II. The error bars include measured differences from multiple samples of the same composition as well as different thermal cycles. No error bars are shown for the data from a single sample since they are negligible in such measurements.

relation,  $\text{volume difference}(\%) = 4.01 - 1.77d_{crit} + 0.048d_{crit}^2$  ( $d_{crit}$  is in mm), with an  $R^2 = 0.67$ . Although not a perfect fit, these data show a semiquantitative correlation with the correct trend that the better glass formers have lesser volumes (more compact) than the estimates from their constituent elements. It is likely that the minimum in the polynomial fit is not real, but an artifact of the fitting procedure that arises from the scatter in the data.

## B. Liquid thermal expansion coefficients

A correlation between thermal expansion coefficient of the transition-metal based liquids and their cohesive energies was established quite early on [29]. Later, a connection between the expansion coefficient and liquid fragility was reported [9]. Since then, measurements on more alloy liquids have been performed. To place the earlier observations on a firmer footing, the expansion coefficients of 41 alloy liquids and their cohesive energies and fragilities are shown in Figs. 3(a) and 3(b), respectively; the corresponding data are listed in Tables I and II. The cohesive energies were estimated from those of the elements [30] and their heats of mixing [28]. Although such estimates correspond to values at absolute zero K, considering that the average specific heat of liquids to be about 30–40 J/mol [31]), the typical enthalpy difference between  $T_l$  and 0 K is expected to be 5–10% smaller than that at 0 K. Within this uncertainty, the data clearly demonstrate a strong correlation between the thermal expansion coefficient and the cohesive energy and liquid fragility, confirming earlier observations [9,29]. It should be noted that we have also compared the expansion coefficient with the bond energy estimated from the cohesive energy and coordination number calculated from

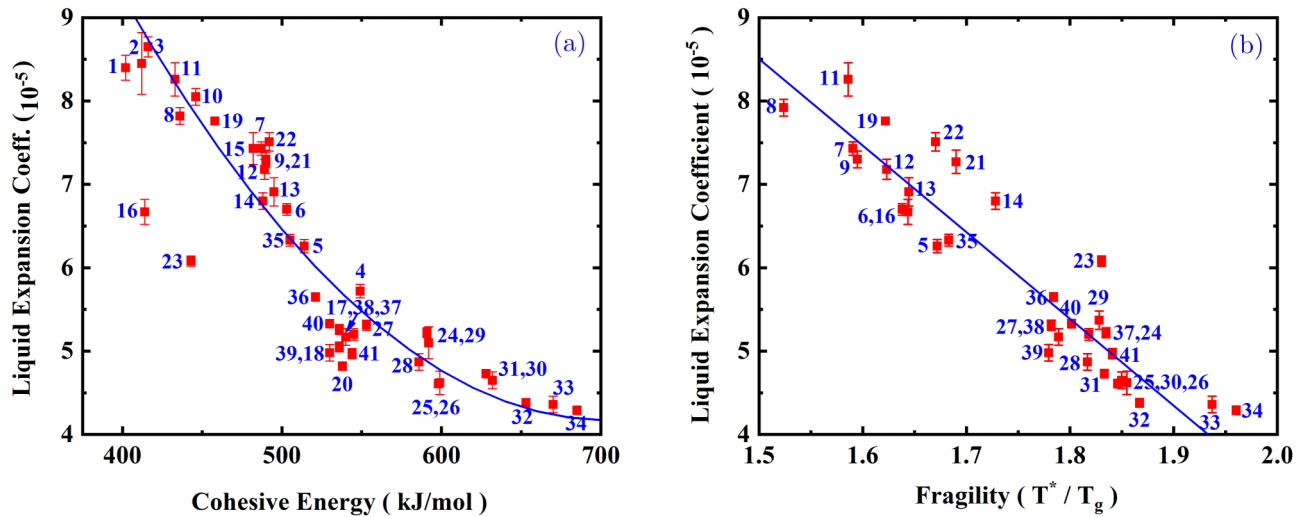


FIG. 3. The liquid expansion coefficient as a function of cohesive energy (a) and fragility (b). The alloy numbers are the same as in Tables I and II. The fit parameters are provided in the text.

the pair-correlation function,  $g(r)$ . The essential result remains unchanged since the coordination number varies little (12–14) across the whole alloy series [32]. A theoretical basis for the correlation between thermal expansion coefficient and fragility will be discussed later.

The data show that stronger liquids (larger  $T^*/T_g$ ) have stronger atomic bonds and smaller thermal expansion coefficients. A polynomial fit to the data in Fig. 3(a) is given by  $\alpha_{\text{liq}}(10^{-5}) = 31.5 - 0.078E + 5.5 \times 10^{-5}E^2$ , where  $E$  is the cohesive energy (kJ/mol). A linear fit to the fragility parameter,  $T^*/T_g$ , in Fig. 3(b) is given by  $\alpha_{\text{liq}}(10^{-5}) = 24.1 - 10.4T^*/T_g$ ;  $R^2 = 0.90$  in both cases. Although  $\alpha_{\text{liq}}$  is one parameter in Eq. (2), a direct connection between this and glass formability is neither expected nor observed. As will be shown below, it is the difference of  $\alpha_{\text{liq}}$  with some base parameter that is important for GFA.

There are two outliers in Fig. 3(a), alloy number 16 ( $\text{Pd}_{82}\text{Si}_{18}$ ) and 23 ( $\text{Y}_{68.9}\text{Co}_{31.1}$ ). One of them contains Si and the other a rare-earth element. It is not clear whether this is indicative of a different type of correlation for the rare-earth and tetrahedrally bonded liquids. In Fig. 3(b), however, alloy number 16 falls in line with the rest of the liquids; alloy number 23 also comes closer to the rest of the liquids.

To probe a connection between the thermal expansion coefficient and GFA, the differences between  $\alpha_{\text{liq}}$  and  $\alpha_{\text{cryst}}$  are compared with  $d_{\text{crit}}$  for the BMGs for which  $\alpha_{\text{cryst}}$  has been measured. When making such comparisons, a few points should be considered. Unlike crystals, where the thermal expansivity is determined by the anharmonicity, the corresponding quantities in the liquids depend not only on the anharmonic contributions but also on the structural changes with temperature. Since most of the BMGs crystallize into a mixture of phases, the anharmonic contributions to the expansion coefficients for the crystal and liquid phases are not expected to be identical. Neglecting such differences, the excess expansivity of the liquid compared to the crystal should then reflect mostly the structural/configurational

changes on melting. Figure 4 shows that this metric decreases linearly with increasing  $d_{\text{crit}}$  following the relation  $(\alpha_{\text{liq}} - \alpha_{\text{cryst}})/\alpha_{\text{cryst}}(\%) = 9.7 - 0.59 d_{\text{crit}}$  (mm) with an  $R^2 = 0.74$ . Therefore, the configurational changes with temperature for the better glass formers are smaller. This is consistent with the observation [9,33] that the structural changes with temperature are smaller for the stronger liquids. The correlation between thermal expansion differences and  $d_{\text{crit}}$  appears to be better than for volume changes on melting (Fig. 1), perhaps, because the difference,  $\alpha_{\text{liq}} - \alpha_{\text{cryst}}$  is a much larger quantity than the difference in their respective volumes and, therefore, can be measured with a higher precision.

As in the case of the volume, the estimated  $\alpha_{\text{liq estm}}$  from the expansion coefficients of the elemental liquids using the

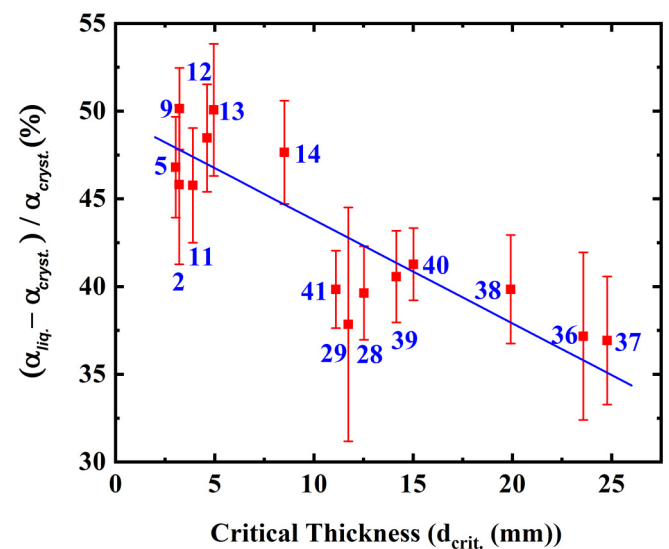


FIG. 4. The difference in the thermal expansion coefficients of the liquids and crystals as a function of critical thickness for 15 BMGs. The linear fit parameters are provided in the text.

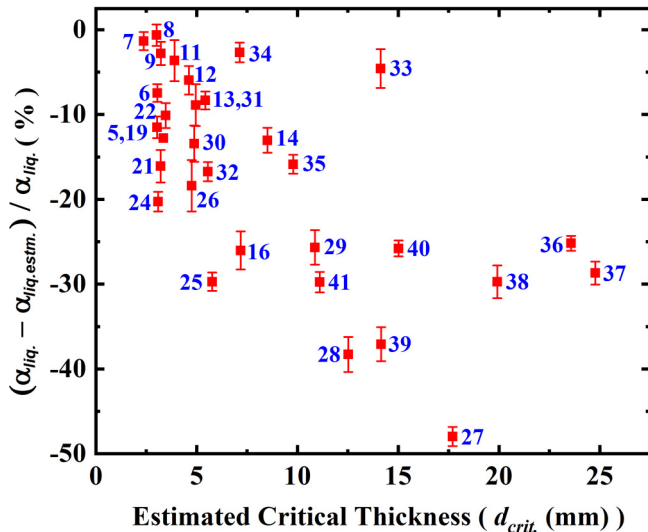


FIG. 5. Difference between the experimentally measured ( $\alpha_{\text{liq}}$ ) and estimated ( $\alpha_{\text{liq,estm.}}$ ) liquid thermal expansion coefficients from the elemental liquids, as a function of estimated critical thicknesses. The parameters and alloy numbers are listed in Tables I and II.

mixing rule was used as another baseline. Since the expansion coefficient of a liquid is nearly temperature independent, unlike for volume, temperature does not come into play in such estimates. To include as many data points as possible, this difference was then compared with the estimated  $d_{\text{crit}}$  by using Eq. (2). This was possible for 31 of the 41 liquids studied (Table II). Figure 5 shows this comparison. Due to a large scatter in the data, no fit was attempted. In spite of this, the general trend is that the difference in expansivity of the liquid and its constituting elements is larger for larger  $d_{\text{crit}}$  and smaller for smaller  $d_{\text{crit}}$ . Due to a large negative heat of mixing for most of the alloys, the alloy expansion coefficient is smaller than those of the elemental liquids (the difference is negative in sign). There is one important difference while considering  $\alpha_{\text{liq}} - \alpha_{\text{cryst}}$  and  $\alpha_{\text{liq}} - \alpha_{\text{liq,estm.}}$ . In the former case, the difference is primarily due to structural/configurational contribution, while in the latter case both anharmonicity and structural changes contribute. A much larger scatter of the data in Fig. 5 is indicative of the complicated ways the two factors contribute to this difference. Clearly,  $\alpha_{\text{liq}} - \alpha_{\text{liq,estm.}}$  does not follow a universal behavior, other than showing a trend. Finally, comparing Fig. 2 for volume and Fig. 5 for thermal expansivity, it is clear that the change in the thermal expansivities on alloying is much larger than in the corresponding volumes.

#### IV. DISCUSSION

Since this study focuses on establishing a connection between volume, thermal expansion, and GFA, the discussion should start with some clear understanding of how GFA is connected with those properties. As mentioned in the Introduction, instead of their magnitudes, only relative changes are important. The magnitude of the thermal expansion coefficient is connected with another property, the liquid fragility, as has

been demonstrated in Figs. 3(a) and 3(b). It has been argued [34] that the fragility is determined by both a rise in the high-frequency shear modulus due to anharmonicity [35] and a growing length scale for the cooperative dynamics [36] with decreasing temperature. The thermal expansion coefficient is also determined by both anharmonicity and the changes in liquid structure/configurations (i.e., change in cooperativity) with temperature. Therefore, a strong correlation between the thermal expansion coefficient and fragility is expected. The data also demonstrate that the fragility, to a large extent, is determined by the strength of the atomic bonds (cohesive energy). Such a connection between atomic bonds, fragility, and thermal expansion coefficient is not widely recognized.

Since efficient packing of atoms is a key ingredient in many theories of metallic glass formation, a connection between volume and GFA is expected. Moreover, the GFA is determined by both the fragility and  $T_{rg}$  [25]. Our recent work showed that instead of  $T_{rg}$ ,  $\alpha_{\text{liq}}$  may be used [14,17]. The two formalisms are essentially similar since  $T_{rg}$  determines the temperature window over which cooperative rearrangements may grow before glass transition, whereas  $\alpha_{\text{liq}}$  determines the effective changes in volume over the same temperature interval. Therefore, a natural connection between  $\alpha_{\text{liq}}$  and GFA is expected.

Our data show that the differences in volume between the liquid and the corresponding crystal are smaller for the better glass formers (Fig. 1). This difference measures the change in atomic configuration on melting, which is smaller for the better glass formers. It demonstrates that the atomic packings in these liquids are closer to those of the crystals, which is consistent with the DRP models [2–5] and experimental data for a few alloys [8], but in conflict with the results of Ref. [6]. The differences in the specific volumes between the alloy liquids and the constituent elements also show some correlation with the GFA ( $d_{\text{crit}}$ ) (Fig. 2). However, since this quantity measures both the changes in anharmonicity and structural contributions compared to those for the elemental liquids, its interpretation is a little more difficult. Negative values for this difference for most of the alloys reflect the effect of strong negative heats of mixing [28]. This appears to be larger for the better glass formers. This is not surprising since most of the good metallic glasses were discovered following the principles suggested by Inoue [27]. However, this quantity does not correlate with the fragility (not shown) since it reflects only the relative changes in the anharmonicity and cooperativity with the corresponding elemental liquids, not their total contributions to the liquid.

The thermal expansion is due to an increase in the anharmonicity with increasing temperature. In liquids, an additional contribution comes from the changes in the liquid structure/configuration with temperature. It has been reported that the differences in vibrational contributions to the entropies in crystals and two metallic glasses,  $\text{Cu}_{50}\text{Zr}_{50}$  and  $\text{Cu}_{46}\text{Zr}_{46}\text{Al}_8$ , are less than 5% [37]. Therefore, when the difference in the expansion coefficients of the liquid and the crystal is considered, it is indicative of the changes in the configurational contributions to the expansivity, especially when the transformation is polymorphic. The data in Fig. 4 demonstrate that the configurational changes are smaller for the better glass



formers. A similar conclusion was drawn from the change in volume on melting. This is consistent with the structural studies, where smaller structural changes with temperature were observed for the stronger liquids [9,33]. All these results give a consistent picture that the GFA is determined by the configurational changes in the liquid.

The differences in thermal expansion coefficients between the alloys and elemental liquids also correlate well with the GFA, but in a nonuniversal manner (likely different for alloys with different base elements). The anharmonic contribution to the thermal expansion coefficient in alloys cannot be considered the same as in the elemental liquids. As mentioned earlier, all liquids in the present study are made from alloys with fairly large negative heats of mixing. Therefore, the attractive part of the interatomic potential is stronger in the alloys. This increases the depth of the interatomic potential and strengthens the atomic bonds. However, how that changes the anharmonicity is a debatable point [36,38–40]. Some studies indicate that a stiffer potential (faster rise in the repulsive part) decreases anharmonicity and the thermal expansion coefficient [38,39]. Others claim that a softer potential (slower rise in the repulsive part) decreases anharmonicity and the thermal expansion coefficient [36,40]. The present data (Fig. 5) indicate that the anharmonicity is reduced by a stronger chemical attraction in the alloy liquids. Most of the Cu-based alloys with smaller negative heat of mixing [28] show smaller decreases, while most of the Zr-based liquids with larger heats of mixing show larger decreases in the expansion coefficients compared to the elemental liquids. This is likely due to the combined effects of anharmonicity and the structural contribution to the expansion coefficient, compared with the elemental liquids. Structural data for the alloys [9] show smaller rates of change of the liquid structures with temperature compared with the elemental liquids [18].

Finally, we emphasize that the data used in this study are confined mostly to early- and late transition-metal based alloys, which are only a small fraction of the large number of metallic glasses discovered thus far. This is clearly a limitation due to the lack of reliable experimental data. Considering the small changes of many of the properties discussed above, it is not a very productive exercise to use data for different properties from different groups; very few studies report data on all of the necessary properties from the same laboratory. Contradictory data for  $d_{\text{crit}}$  in the literature are one such example [24,25]. This is why we restricted ourselves to estimated values of the critical thicknesses. Although not precise, our estimated values provide some consistency. Measurements of high-temperature liquid properties are not easy, especially the thermal expansion coefficient and viscosity of high vapor pressure liquids, such as those containing rare-earth and alkaline-earth metals. Surface contamination even under high vacuum makes it impossible to perform such measurements in many cases, especially for the viscosity.

## V. CONCLUSION

A number of conclusions may be derived from the results of this study. First, it is clear that the absolute values of density/volume and thermal expansion coefficients are not true metrics for assessing the GFA; relative changes with some baseline are the more relevant parameters. Although several models have been developed to understand liquid dynamics and glass formation based on free volumes [41,42], from a practical viewpoint, it is probably a difficult metric to get valuable insights. It is well recognized that even for the elemental liquids, the volume/density change on melting is small, only a few percent [43]. As demonstrated here, whether they are good or poor glass formers, the volume change on melting is smaller than 2%. Therefore, any observable effect of volume on GFA will require very high-precision measurements. This appears to be impractical for the BMGs, especially because of their high melting temperatures. Instead, the thermal expansion coefficient is a better metric, when compared with a proper baseline, for GFA ( $d_{\text{crit}}$ ). This property can be measured with a much higher precision using the containerless processing techniques. Therefore, it is emphasized that the changes in the expansion coefficient with alloying, instead of volume, are much better indicators of glass formability. The results are consistent with efficient packing of atoms in good glass-forming alloys.

It is our hope that more studies on a more diverse class of BMGs will be made to verify these conclusions. Given the experimental difficulties, computer simulation studies, such as molecular dynamics, may also be useful. Since the equilibrium/near-equilibrium properties of the high-temperature liquids are used in this exercise, such studies will be reliable. Unlike its inherent limitations for the studies of metastable liquids, equilibrium liquids do not require prohibitive computational costs and the relaxation rates in the simulations and the real liquids are of the same order. However, developing reliable interatomic potential for each alloy is an enormous exercise, especially when it is known that small changes in composition or small additions often change the properties of the BMGs significantly. Although significant amounts of simulation studies exist in the literature, to the best of our knowledge, no concerted effort has been made to test correlations for a large number of metallic liquids, as has been undertaken in this experimental study.

## ACKNOWLEDGMENTS

This work was partially supported by NASA under Grants No. NNX10AU19G and No. NNX16AB52G.

Any opinions, findings, and conclusions or recommendations expressed in this material are those of the author(s) and do not necessarily reflect the views of NASA.

[1] W. J. Klement, R. H. Wilens, and P. Duwez, *Nature (London)* **187**, 869 (1960).

[2] J. D. Bernal, *Proc. R. Soc. London A* **280**, 299 (1964).

[3] H. W. Sheng, W. K. Luo, F. M. Alamgir, J. M. Bai, and E. Ma, *Nature (London)* **439**, 419 (2006).

[4] E. Ma, *Nat. Mater.* **14**, 547 (2015).

- [5] D. B. Miracle, *Nat. Mater.* **3**, 697 (2004).
- [6] Y. Li, Q. Guo, J. A. Kalb, and C. V. Thompson, *Science* **322**, 1816 (2008).
- [7] J. C. Bendert, A. K. Gangopadhyay, N. A. Mauro, and K. F. Kelton, *Phys. Rev. Lett.* **109**, 185901 (2012).
- [8] S. Mukherjee, J. Schroers, Z. Zhou, W.L. Johnson, and W.-R. Rhim, *Acta Mater* **52**, 3689 (2004).
- [9] A. K. Gangopadhyay, C. E. Pueblo, R. Dai, M. L. Johnson, R. Ashcraft, D. Van Hoesen, M. Sellers, and K. F. Kelton, *J. Chem. Phys.* **146**, 154506 (2017).
- [10] A. K. Gangopadhyay, G. W. Lee, K. F. Kelton, J. R. Rogers, A. I. Goldman, D. S. Robinson, T. J. Rathz, and R. W. Hyers, *Rev. Sci. Instrum.* **76**, 073901 (2005).
- [11] N. A. Mauro and K. F. Kelton, *Rev. Sci. Instrum.* **82**, 035114 (2011).
- [12] W.-K. Rhim, M. Collender, M. T. Hyson, W. T. Simms, and D. D. Elleman, *Rev. Sci. Instrum.* **56**, 307 (1985).
- [13] R. C. Bradshaw, J. R. Rogers, K. F. Kelton, R. W. Hyers, and D. P. Schmidt, *Rev. Sci. Instrum.* **76**, 125108 (2005).
- [14] R. Dai, R. Ashcraft, A. K. Gangopadhyay, and K. F. Kelton, *J. Non-Cryst. Solids* **525**, 119673 (2019).
- [15] C. A. Angell, *J. Phys. Chem. Solids* **49**, 863 (1988).
- [16] W.-K. Rhim, K. Ohsaka, P.-F. Paradis, and R. E. Spjut, *Rev. Sci. Instrum.* **70**, 2796 (1999).
- [17] R. Dai, A. K. Gangopadhyay, R. J. Chang, and K. F. Kelton, *Acta Mater.* **172**, 1 (2019).
- [18] A. K. Gangopadhyay and K. F. Kelton, *J. Non-Cryst. Solids: X* **2**, 100016 (2019).
- [19] T. Iwashita, D. M. Nicholson, and T. Egami, *Phys. Rev. Lett.* **110**, 205504 (2013).
- [20] Y. Fan, T. Iwashita, and T. Egami, *Phys. Rev. Lett.* **115**, 045501 (2015).
- [21] M. E. Blodgett, T. Egami, Z. Nussinov, and K. F. Kelton, *Sci. Rep.* **5**, 13837 (2015).
- [22] A. Jaiswal, T. Egami, K. F. Kelton, K. S. Schweizer, and Y. Zhang, *Phys. Rev. Lett.* **117**, 205701 (2016).
- [23] A. K. Gangopadhyay and K. F. Kelton, *J. Mater. Res.* **32**, 2638 (2017).
- [24] H. W. Kui, A. L. Greer, and D. Turnbull, *Appl. Phys. Lett.* **45**, 615 (1984).
- [25] W. L. Johnson, J. H. Na, and M. D. Demitriou, *Nat. Commun.* **7**, 10313 (2016).
- [26] K. F. Kelton, G. W. Lee, A. K. Gangopadhyay, R. W. Hyers, T. J. Rathz, J. R. Rogers, M. B. Robinson, and D. S. Robinson, *Phys. Rev. Lett.* **90**, 195504 (2003).
- [27] A. Inoue, K. Ohtera, A. P. Tsai, and T. Masumoto, *Jpn. J. Appl. Phys.* **27**, L280 (1988).
- [28] F. R. de Boer, R. Boom, W. C. M. Mattens, A. R. Miedema, and A. K. Niessen, *Cohesion in Metals-Transition Metal Alloys* (North-Holland, Amsterdam, 1988).
- [29] A. K. Gangopadhyay, J.C. Bendert, N. A. Mauro, and K. F. Kelton, *J. Phys.: Condens. Matter.* **24**, 375102 (2012).
- [30] C. Kittel, *Introduction to Solid State Physics*, 7th ed. (Wiley, New York, 1996), p. 57.
- [31] *Smithells Metals Reference Book*, edited by E. A. Brandes and G. B. Brook, 7th ed. (Butterworth-Heinemann, Oxford, 1992).
- [32] A. K. Gangopadhyay, M. E. Blodgett, M. L. Johnson, J. McKnight, V. Wessels, A. J. Vogt, N. A. Mauro, J. C. Bendert, R. Soklaski, L. Yang, and K. F. Kelton, *J. Chem. Phys.* **140**, 044505 (2014).
- [33] D. N. Voylov, P. J. Griffin, B. Mercado, J. K. Keum, M. Nakanishi, V. N. Novikov, and A. P. Sokolov, *Phys. Rev. E* **94**, 060603(R) (2016).
- [34] J. C. Dyre, *Rev. Mod. Phys.* **78**, 953 (2006).
- [35] Th. Bauer, P. Lunkenheimer, and A. Loidl, *Phys. Rev. Lett.* **111**, 225702 (2013).
- [36] J. Mattsson, H. M. Wyss, A. Fernandez-Nieves, K. Miyazaki, Z. Hu, D. R. Reichman, and D. A. Weitz, *Nature (London)* **462**, 83 (2009).
- [37] H. L. Smith, Chen W. Li, A. Ho, G. R. Garrett, D. S. Kim, F. C. Yang, M. S. Lucas, T. Swan-Wood, J. Y. Y. Lin, M. B. Stone, D. L. Abernathy, M. D. Demetriou, and B. Fultz, *Nat. Phys.* **13**, 900 (2017).
- [38] C. E. Pueblo, M. Sun, and K. F. Kelton, *Nat. Mater.* **16**, 792 (2017).
- [39] P. Bordat, F. Affouard, M. Descamps, and K. L. Ngai, *Phys. Rev. Lett.* **93**, 105502 (2004).
- [40] R. Casalini, *J. Chem. Phys.* **137**, 204904 (2012).
- [41] M. H. Cohen and D. Turnbull, *J. Chem. Phys.* **31**, 1164 (1959).
- [42] M. H. Cohen and G. S. Grest, *Phys. Rev. B* **20**, 1077 (1979).
- [43] T. Iida and R. I. L. Guthrie, *The Physical Properties of Liquid Metals* (Clarendon, Oxford, 1988).
- [44] M. J. Assael, K. Kakosimos, R. M. Banish, J. Brillo, I. Egry, R. Brooks, P. N. Quedstedt, K. C. Mills, A. Nagashima, Y. Sato, and W. A. Wakeham, *J. Phys. Chem. Ref. Data* **35**, 285 (2006).
- [45] V. Sarou-Kanian, F. Millot, and J. C. Rifflet, *Int. J. Thermophys.* **24**, 277 (2003).
- [46] M. J. Assael, I. J. Armyra, J. Brillo, S. V. Stankus, J. Wu, and W. A. Wakeham, *J. Phys. Chem. Ref. Data* **41**, 033101 (2012).
- [47] M. J. Assael, A. E. Kalyva, K. D. Antoniadis, R. M. Banish, I. Egry, J. Wu, E. Kaschnitz, and W. A. Wakeham, *J. Phys. Chem. Ref. Dta* **39**, 033105 (2010).
- [48] J. Brillo and I. Egry, *Int. J. Thermophys.* **24**, 1155 (2003).
- [49] P.-F. Paradis, T. Ishikawa, and J. T. Okada, *Johnson Matthey Tech. Rev.* **58**, 124 (2014).
- [50] H. Yoo, C. Park, S. Jeon, S. Lee, and G. W. Lee, *Metrologia* **52**, 677 (2015).
- [51] P.-F. Paradis, T. Ishikawa, Y. Saita, and S. Yoda, *Int. J. Thermophys.* **25**, 1905 (2004).
- [52] Y. Sato, T. Nishizuka, K. Hara, T. Yamamura, and Y. Waseda, *Int. J. Thermophys.* **21**, 1463 (2000).
- [53] P.-F. Paradis and W. -K. Rhim, *J. Chem. Therm.* **32**, 123 (2000).
- [54] T. Ishikawa, P.-F. Paradis, T. Itami, and S. Yoda, *J. Chem. Phys.* **118**, 7912 (2003).
- [55] P.-F. Paradis, T. Ishikawa, and N. Koike, *Micrograv. Sci. Tech.* **21**, 113 (2009).
- [56] C. Chattopadhyay, K. S. N. Satish Idury, J. Bhatt, K. Mondal, and B. S. Murty, *Mater. Sci. Technol.* **32**, 380 (2016).
- [57] W. H. Wang, J. J. Lewandowski, and A. L. Greer, *J. Mater. Res.* **20**, 2307 (2005).
- [58] D. Wang, Y. Li, B. B. Sun, M. L. Sui, K. Lu, and E. Ma, *Appl. Phys. Lett.* **84**, 4029 (2004).
- [59] D. Xu, B. Lohwongwatana, G. Duan, W. L. Johnson, and C. Garland, *Acta Mater.* **52**, 2621 (2004).
- [60] H. Men, S. J. Pang, and T. Zhang, *Mater. Sci. Eng. A* **408**, 326 (2005).
- [61] A. Inoue, W. Zhang, T. Zhang, and K. Kurosoka, *Acta Mater.* **49**, 2645 (2001).

- [62] A. Inoue and W. Zhang, *Mater. Trans.* **43**, 2921 (2002).
- [63] H. B. Yu, W. H. Wang, and H. Y. Bai, *Appl. Phys. Lett.* **96**, 081902 (2010).
- [64] D. Xu, G. Duan, and W. L. Johnson, *Phys. Rev. Lett.* **92**, 245504 (2004).
- [65] K. F. Yao, F. Ruan, Y. Q. Yang, and N. Chen, *Appl. Phys. Lett.* **88**, 122106 (2006).
- [66] X. H. Lin and W. L. Johnson, *J. Appl. Phys.* **78**, 6514 (1995).
- [67] S. L. Zhu, X. M. Wang, F. X. Qin, and A. Inoue, *Mater. Sci. Eng. A* **459**, 233 (2007).
- [68] T. Wada, F. Qin, X. Wang, M. Yoshimura, A. Inoue, N. Sugiyama, R. Ito, and N. Matsushita, *J. Mater. Res.* **24**, 2941 (2009).
- [69] Y. H. Li, W. Zhang, C. Dong, J. B. Qiang, A. Makino, and A. Inoue, *Intermetallics* **18**, 1851 (2010).
- [70] H. Cao, D. Ma, K.-C. Hsieh, L. Ding, W. G. Stratton, P. M. Voyles, Y. Pan, M. Cai, J. T. Dickinson, and Y. A. Chang, *Acta Mater.* **54**, 2975 (2006).
- [71] A. Inoue, T. Zhang, N. Nishiyama, K. Ohba, and T. Mashumoto, *Mater. Trans. JIM* **34**, 1234 (1993).